RSC Chemical Biology

ROYAL SOCIETY OF CHEMISTRY

PAPER

View Article Online
View Journal | View Issue

Cite this: *RSC Chem. Biol.*, 2024, **5**, 1045

Capture of RNA G-quadruplex structures using an L-RNA aptamer†

Sin Yu Lam, ‡[a] Mubarak Ishaq Umar,‡[ab] Haizhou Zhao,[a] Jieyu Zhao[a] and Chun Kit Kwok *[ac]

G-quadruplexes (dG4 and rG4) are nucleic acid secondary structures formed by the self-assembly of certain G-rich sequences, and they have distinctive chemical properties and play crucial roles in fundamental biological processes. Small molecule G4 ligands were shown to be crucial in characterizing G4s and understanding their functions. Nevertheless, concerns regarding the specificity of these synthetic ligands for further investigation of G4s, especially for rG4 isolation purposes, have been raised. In comparison to G4 ligands, we propose a novel magnetic bead-based pulldown assay that enables the selective capture of general rG4s using functionalized L-Apt.4-1c from both simple buffer and complex media, including total RNA and the cell lysate. We found that our L-RNA aptamer can pulldown general rG4s with a higher efficiency and specificity than the G4 small molecule ligand BioTASQ v.1 in the presence of non-target competitors, including dG4 and non-G4 structures. Our findings reveal that biotinylated L-aptamers can serve as effective molecular tools for the affinity-based enrichment of rG4 of interest using this new assay, which was also verified by quantitative reverse transcription-polymerase chain reaction (RT-qPCR) on endogenous transcripts. This work provides new and important insights into rG4 isolation using a functionalized L-aptamer, which can potentially be applied in a transcript-specific or transcriptome-wide manner in the future.

Received 12th July 2024,
Accepted 13th August 2024

DOI: 10.1039/d4cb00161c

rsc.li/rsc-chembio

Introduction

RNA G-quadruplexes (rG4s) are non-canonical secondary structures that form through association of guanine (G)-rich RNA sequences. Four guanine bases (Gs) interact with each other to form square planar G-quartet structures (Fig. 1A), which stack to form G-quadruplex (G4) structures (Fig. 1B). These structures are stabilized in the presence of central monovalent cations ($K^+ > Na^+ > Li^+$).[1,2] G-quadruplexes (G4s) are thermostable and play vital roles in various cellular activities, including replication, transcription, and translation, in diverse organisms, encompassing humans, mice, plants, viruses, yeasts, and bacteria.[3–9] Due to their biological significance, G4s have been recognized as promising targets in cancer research and antimicrobial studies.[10,11] Targeting G4s is crucial for studying their cellular roles,[12] and over the years, several classes of G4 targeting tools have been developed, which include G4-specific antibodies, peptides, and chemicals.[13]

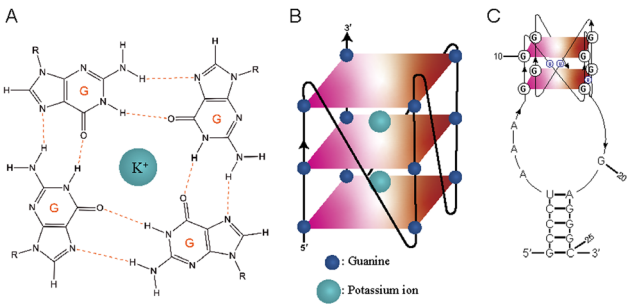

Fig. 1 G-quartet and G-quadruplex (G4) structures and the L-RNA aptamer used in this study. (A) Chemical structure of a G-quartet together with a central monovalent cation, with the strength of stability in the order ($K^+ > Na^+ > Li^+$). (B) G-quadruplex (G4) is formed by stacking two or more G-quartets. (C) G-rich sequence of L-Apt.4-1c is folded into two G-quartet rG4 structures.

Among the G4 targeting tools mentioned above, several G4-specific tools have shown high affinity for G4s (dG4s and rG4) and are useful for stabilizing and characterizing them.[14–18] These tools include antibodies like BG4 and 1H6 as well as peptides like cyclic RHAU23, b-G4pep3, and pep11.[19–22] Small molecule G4 ligands, such as *N*-methyl mesoporphyrin IX

[a] *Department of Chemistry and State Key Laboratory of Marine Pollution, City University of Hong Kong, Kowloon Tong, Hong Kong SAR 999077, China*
[b] *RNA Molecular Biology Group, National Institute of Arthritis and Musculoskeletal and Skin Diseases (NIAMS), National Institutes of Health, Bethesda, MD, USA*
[c] *Shenzhen Research Institute of City University of Hong Kong, Shenzhen, China. E-mail: ckkwok42@cityu.edu.hk*

† Electronic supplementary information (ESI) available. See DOI: https://doi.org/10.1039/d4cb00161c

‡ These authors contributed equally.

(NMM), QUMA-1, and Thioflavin T (ThT), have also demonstrated preferential binding to both DNA and RNA G4s.[23–25] They are widely used for G4 detection due to their ability to increase fluorescence intensity upon binding. Pyridostatin (PDS) is an example that has been reported to stabilize telomeric G4 and subsequently disrupt the telomerase activity of human cells.[26] Template-assembled synthetic G-quartets (TASQs) are biomimetic ligands that target G4s and have been extensively studied and evolved into different variants like CyTASQ, BioTASQ, and BioCyTASQ,[27] having applications in G4 isolation, visualization and imaging systems.[28,29] Müller *et al.*[12] and Sperti *et al.*[30] performed *in vitro* G4 pull-down using the biotinylated PDS and TASQs, respectively, for further investigation of G4s. While these studies have been significant in advancing G4 ligands as molecular tools for G4s, it is important to note that these G4 ligands cannot readily distinguish dG4 and rG4 targets. Additionally, the synthesis and preparation of some of the G4 ligands can be challenging, presenting a critical bottleneck for further development and application of G4 tools, as well as general characterization of G4s. As a potential solution and application, we propose an alternative strategy for targeting specific rG4s, which involves the use of L-RNA aptamers.

Aptamers are short, single-stranded DNA or RNA oligonucleotides that bind to their target of interest with high affinity and specificity.[31,32] Natural aptamers (D-oligonucleotides) are prone to nuclease-mediated degradation in biological media.[33,34] To overcome this issue, modified aptamers have been developed using a mirror-image SELEX selection process that eventually generates unnatural L-DNA/L-RNA aptamers that have great biostability.[35–37] Our group previously selected and reported a series of novel L-RNA aptamers, including L-Ap3-7,[38] L-Apt.4-1c,[39] and L-Apt.8f[40] through rG4-SELEX for targeting *TERRA* rG4, *hTERC* rG4, and *APP* rG4, respectively. These L-aptamers exhibited great binding affinity to their targets and high specificity over dG4s and non-G4s as shown in previous studies. To address the specificity limitation of traditional G4 ligands, L-aptamers offer advantages such as high rG4 specificity, ease of synthesis, low cytotoxicity and low immunogenicity.[31] These advantages make L-aptamers a promising alternative in our proposed approach for further rG4 research. Among these L-aptamers, L-Apt.4-1c is the shortest L-RNA aptamer developed so far with 25 nucleotides, exhibiting high affinity binding to D-*hTERC* rG4 and preferential binding to rG4s, but not to dG4s and non-G4s. Our structural analysis also suggested that the G-rich regions of the aptamer folds into a unique two G-quartet rG4 structure (Fig. 1C).[39,41] Herein, we introduce a novel pulldown approach for isolating a specific rG4 *in vitro* using L-Apt.4-1c from both simple buffer and complex biological media, including total RNA and the cell lysate. This aptamer has great potential to serve as a substitute for G4 ligands for certain applications related to rG4s. We report that the pulldown efficiency of L-Apt.4-1c is high for a specific rG4 in both the absence and the presence of different non-targets. Notably, our results demonstrate that L-Apt.4-1c is highly effective in isolating rG4 of interest, and its performance is better compared to the G4 small molecule ligand BioTASQ v.1.

Results and discussion

Design of pulldown assay

Our group recently reported that L-Apt.4-1c exhibits high affinity for general D-rG4s, such as D-*NRAS* rG4, D-*APP* rG4, and D-*hTERC* rG4. Among these rG4s, D-*hTERC* rG4 was a positive target of L-Apt.4-1c in rG4-SELEX, with a dissociation constant (K_d) of 59.1 ± 11.9 nM.[39] To investigate whether L-RNA aptamers can serve as molecular tools that have equal or even superior performance to G4 ligands, we designed a novel pulldown assay (both non-competitive and competitive) to specifically pulldown FAM-D-rG4 targets using streptavidin-coated magnetic beads (SA-MBs) coupled with Biotin-l-Apt.4-1c (Fig. 2). We first appended the biotin label at the 5′ position of L-Apt.4-1c as the biotin functional group is needed for interacting with the streptavidin-coated magnetic beads for pulldown purposes. To evaluate the impact of biotin labeling of L-Apt.4-1c on the binding affinity towards 5′-FAM-D-*hTERC* rG4, we conducted a binding experiment using MST, and determined the K_d value to be 72.2 ± 14.6 nM (Fig. S1, ESI†). This K_d value is comparable to the value obtained from the unlabelled L-Apt.4-1c and FAM-D-*hTERC* rG4 interaction, indicating that the functionalization of L-Apt.4-1c with 5′-biotin does not affect its interaction with D-*hTERC* rG4, and thus we can use it for the development of the pulldown assay. To investigate whether other FAM-D-rG4 targets are also feasible in our pulldown assay, we selected FAM-D-*NRAS* rG4 and FAM-D-*APP* rG4 as two additional rG4s, with the K_d values of 75.0 ± 10.2 nM (Fig. S2, ESI†) and 55.8 ± 4.52 nM (Fig. S3, ESI†) towards Biotin-L-Apt.4-1c, respectively.

For this new pulldown assay, we have devised the workflow as follows: first, FAM-D-rG4 targets (including *hTERC* rG4, *NRAS* rG4, and *APP* rG4) (100 nM) or other non-targets were incubated in 1× annealing buffer with different concentrations of biotinylated substrates (including Biotin-L-Apt.4-1c and BioTASQ v.1): 0 nM, 2.5 nM, 120 nM, 300 nM, 800 nM, and 1600 nM as non-competitive assay (Fig. 2, step 1). Similar experiments were performed using BioTASQ v.1 to compare the pulldown efficiency and specificity for rG4 shown by the biotin-L-RNA aptamer *versus* the G4 small molecule ligand. Next, to ensure that the pulldown of rG4 targets by the Biotin-L-aptamer is not affected by competitors, we performed competitive assay. For competitive assay, FAM-D-*hTERC* rG4 and Biotin-L-Apt.4-1c were incubated with either 1× or 10× unlabelled competitors in step 1 (Fig. S4, ESI†). A few non-targets with different structures were chosen as competitors (including RNA hairpin, *hTELO* dG4 with hybrid topology, and a mixture of poly rA, rU, and rC) due to their lack of binding with Biotin-L-Apt.4-1c. To validate the specificity of the pulldown by the biotin-L-aptamer for rG4, FAM-*hTERC* dG4 was chosen as one of the competitors. FAM-*hTERC* dG4 is the DNA version of FAM-*hTERC* rG4 with parallel topology, which weakly binds to Biotin-L-Apt.4-1c, with a K_d value of 221 ± 57.6 nM (Fig. S5, ESI†). The pulldown assay relies on the biotinylated complex (like Biotin-L-Apt.4-1c–FAM-D-*hTERC* rG4) attachment to yeast tRNA blocked SA-MBs (Fig. 2, step 2). The supernatant

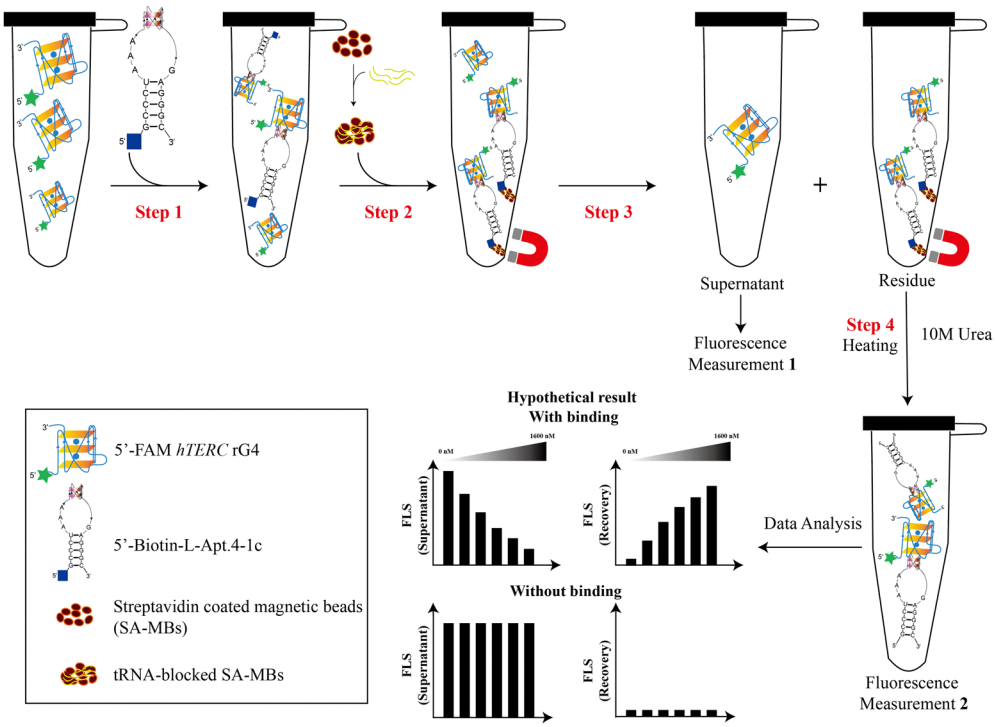

Fig. 2 Schematic illustration of novel *in vitro* magnetic bead-based pulldown assay for rG4s using an rG4-targeting L-RNA aptamer. The 5′-FAM-*hTERC* rG4 (or other rG4s such as FAM-*NRAS* rG4 and FAM-*APP* rG4) and 5′-Biotin-L-Apt.4-1c (L-RNA aptamer) were denatured separately and incubated together (step 1). The reaction mixture is then incubated with the pre-prepared tRNA-blocked streptavidin-coated magnetic beads (step 2), in which the excess or unbound 5′-FAM-*hTERC* rG4 (or other rG4s) was collected in the supernatant and quantified as Measurement 1 (step 3). The product in the residue (rG4 bound L-aptamer) was pulled down and then recovered using 10 M urea and thermal treatment (step 4). The collected residue was quantified as Measurement 2. For a non-competitive pulldown approach, the 5′-Biotin-L-Apt.4-1c was incubated with other 5′-FAM non-targets (including *hTELO* dG4 and RNA hairpin) and *hTERC* dG4 (DNA form of *hTERC* rG4) using the same procedures as described above.

(unbound FAM-labelled target) was eluted from the biotinylated bound complex (residue) using a magnetic rack upon binding (Fig. 2, step 3). The unbound FAM-labelled supernatant was measured and denoted as Measurement 1 (Fig. 2). Last, the residues (bound) in the magnetic beads were washed with 1× annealing buffer and incubated at 95 °C for 15 minutes with 10 M urea to release biotinylated complexes (bound) (Fig. 2, step 4). Measurement 1 (supernatant) was conducted to ascertain the amount of unbound target or non-target in the presence of 5′-biotin-L-Apt.4-1c, while measurement 2 (recovery) quantified the amount of target or non-target bound to 5′-Biotin-L-Apt.4-1c. The fluorescence intensity was normalized to 100% and more details of the data analysis can be found in the Method section in the ESI.†

Evaluation of the binding capacity of L-Apt.4-1c in a simple buffer

To examine the capacity and specificity of L-Apt.4-1c to pulldown rG4s specifically, we first performed a non-competitive pulldown assay using FAM-non-targets, including RNA hairpin, *hTELO* dG4, and *hTERC* dG4.[39] Based on the data, we observed that both the RNA hairpin (Fig. 3A and B) and *hTELO* dG4 (Fig. 3C and D) cannot be pulled down by the biotin-L-aptamer due to the absence of binding. This was indicated by the steady fluorescence intensity of the supernatant (approximately 100%) and the absence of recovery (approximately 0%). Theoretically, the fluorescence intensity of the supernatant decreased with increasing concentration of the biotin-L-aptamer (Fig. 2) upon binding with its corresponding target. Since FAM-*hTERC* dG4 showed weak binding with Biotin-l-Apt.4-1c (Fig. S5, ESI†), the fluorescence intensity showed an increasing trend, but only recovered to 41.4 ± 1.95% at 1600 nM Biotin-L-Apt.4-1c (Fig. 3E and F). To investigate the effectiveness of the biotin-L-aptamer in isolating the rG4 of interest, we performed a non-competitive assay using FAM-*hTERC* rG4, FAM-NRAS rG4, and FAM-*APP* rG4.[39] *hTERC* rG4 exhibited an approximately 3 times stronger binding affinity than *hTERC* dG4 with Biotin-L-Apt.4-1c. The pulldown product of FAM-*hTERC* rG4-Biotin-L-Apt.4-1c showed a recovery of 4.47 ± 2.60% when the concentration of Biotin-L-Apt.4-1c ranged from 0 to 2.5 nM (Fig. 3G and H). Remarkably, a significant increase in the fluorescence intensity recovery was observed from 4.47 ± 2.60% to 44.3 ± 5.23% within the range of 2.5 to 120 nM, which aligns with the K_d value from MST. As the concentration of Biotin-l-Apt.4-1c exceeded the K_d value from 300 to 1600 nM, there appeared to be a gradual saturation at 67.2 ± 5.38% of the fluorescence intensity with an increasing trend. Similar increasing trends were observed in the pulldown of FAM-*NRAS* rG4 and FAM-*APP* rG4. The fluorescence intensity recovery increased from 24.5 ± 3.10% to 66.1 ± 3.84%

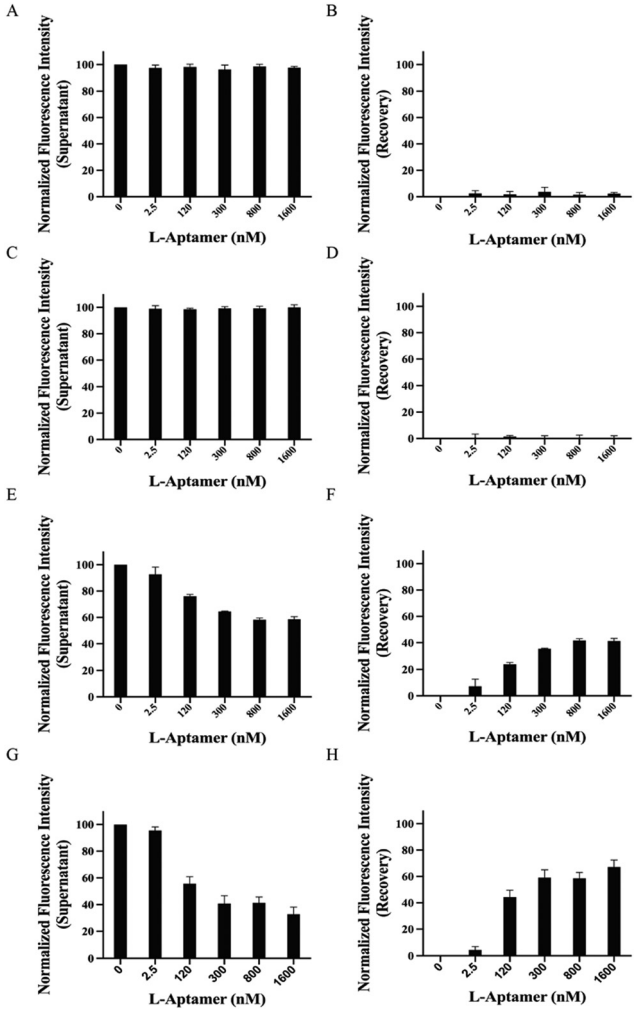

Fig. 3 Pulldown efficiency for FAM-non-targets (non-G4 and dG4s) and the FAM-rG4 target were shown by Biotin-l-Apt.4-1c. The pulldown of FAM-D-targets (100 nM) by Biotin-L-Apt.4-1c (0, 2.5, 120, 300, 800, and 1600 nM) was monitored using the fluorescence intensities and normalized at 100%. Left panels represent the fluorescence intensity of the supernatant, while right panels represent the recovery of fluorescence intensity. Non-competitive pulldown assay using Biotin-L-Apt.4-1c with (A) and (B) FAM-D-RNA hairpin (non-G4 structure), (C) and (D) FAM-D-*hTELO* dG4 (dG4 structure), (E) and (F) FAM-D-*hTERC* dG4 (dG4 structure), and (G) and (H) FAM-D-*hTERC* rG4 (rG4 structure). Biotin-L-Apt.4-1c specifically pulls down the FAM-rG4 target with an obvious decreasing trend in the left panel and increasing trend in the right panel. The pulldown efficiency for the FAM-rG4 target was higher than that for either FAM-D-*hTERC* dG4 (the DNA version of FAM-D-*hTERC* rG4) or other FAM-non-targets (non-G4 and dG4). Error bars indicate the standard deviation from three independent replicates.

(Fig. S6, ESI†) and from 14.6 ± 2.78% to 48.8 ± 3.59% (Fig. S7, ESI†) within the range of 2.5 to 1600 nM, respectively. To avoid false positive results in isolating FAM-rG4s using the biotin-L-aptamer, we conducted a similar set of experiments as a negative control, except that we used Biotin-l-Apt.4-1c M9, which is a mutated version of Biotin-L-Apt.4-1c. Our group conducted the mutagenesis experiment by EMSA and found that some point mutations of this L-aptamer showed no binding, especially the Gs potentially involved in the formation of the G-quartet structure.[39] Among these mutants, we chose the point mutation from G9 to A9 (named Biotin-L-Apt.4-1c M9) for our pulldown assay, which resulted in the absence of an increasing trend as the concentration of Biotin-l-Apt.4-1c M9 was increased (Fig. S8, ESI†). In short, our non-competitive pulldown assay reflected that Biotin-l-Apt.4-1c isolates general rG4s with the highest fluorescence recovery, highlighting the validity of this novel assay and illustrating the capturing ability of this L-aptamer for general rG4s against other non-targets.

To identify whether Biotin-L-Apt.4-1c specifically recognizes general rG4 structures against rG4 mutants, we performed competitive pulldown assays using the biotin-L-aptamer for the isolation of rG4s in the presence of their corresponding rG4 mutants. In each rG4, we mutated some Gs to As in the respective sequences to disrupt the formation of the rG4s (Table S1, ESI†). The fluorescence intensities showed an increasing trend in the recovery and gradually saturated at 1600 nM for the isolation of *hTERC* rG4, *NRAS* rG4, and *APP* rG4 in the presence of their corresponding rG4 mutants, with values of 53.7 ± 5.94% (Fig. S9, ESI†), 61.5 ± 1.57% (Fig. S10, ESI†), and 42.5 ± 2.26% (Fig. S11, ESI†), respectively. The fluorescence recoveries in the presence of rG4 mutants were similar to the non-competitive results, which showed that Biotin-L-Apt.4-1c was able to distinguish between rG4 structures or rG4 mutants to avoid false positive results. To further display the pulldown efficiency of Biotin-L-Apt.4-1c for FAM-*hTERC* rG4 in the presence of non-targets, we employed unlabelled structural and non-structural competitors, including *hTERC* dG4, *hTELO* dG4, and a mixture of poly rA, rC, and rU. The unlabelled non-targets were utilized to compete with FAM-*hTERC* rG4 when incubating with Biotin-L-Apt.4-1c (Fig. S4, ESI†). Meanwhile, to investigate the influence of the structured competitor amount, we used two different ratios of *hTERC* rG4 to non-target dG4s: 1 : 1 (1×) and 1 : 10 (10×). We incubated Biotin-L-Apt.4-1c with FAM-*hTERC* rG4 in the presence of either 1× or 10× unlabelled *hTELO* dG4 or *hTERC* dG4 competitor. Upon binding with the non-targets, the recovery of fluorescence intensity will be approximately 0% due to the absence of the FAM label in the 5′ position. In the presence of the 1× structural competitor, we observed that there is a significant increase in the recovery of fluorescence intensity (3.78 ± 3.53% to 44.9 ± 3.20% and 11.9 ± 2.55% to 50.3 ± 1.68%) within the range of 2.5 to 120 nM Biotin-L-Apt.4-1c upon binding towards FAM-*hTERC* rG4 in the presence of 1× *hTELO* dG4 and 1× *hTERC* dG4, respectively, which gradually reached saturation at 65.1 ± 2.08% and 67.1 ± 2.45% at 1600 nM (Fig. 4 and Fig. S12, ESI†). Similarly, an increasing trend of fluorescence intensity was observed, with 66.6 ± 3.23% and 56.7 ± 16.1% recovered at 1600 nM in the presence of 10× *hTERC* dG4 and 10× *hTELO* dG4, respectively (Fig. S12 and S13, ESI†). Although both *hTELO* dG4 and *hTERC* dG4 serve as dG4 non-targets, FAM-*hTELO* dG4 cannot be pulled down by the biotin-L-aptamer (Fig. 3D), while FAM-*hTERC* dG4 can be pulled down by the biotin-L-aptamer (Fig. 3F). However, the results here showed that the inclusion of the 1× or 10× unlabelled *hTELO* dG4 or *hTERC* dG4 resulted in

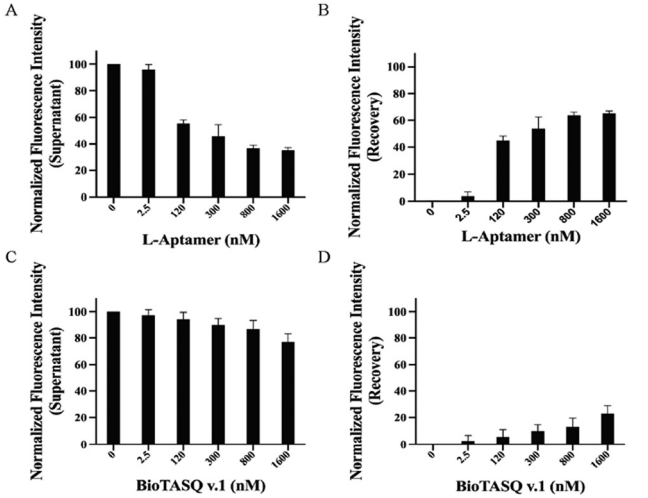

Fig. 4 Pulldown efficiency for FAM-*hTERC* rG4 was shown by the L-aptamer and the G4 small molecule ligand in the presence of a 1× non-target competitor. (A) and (B) Competitive assay of FAM-D-*hTERC* rG4 by biotin-L-Apt.4-1c in the presence of a 1× unlabelled D-*hTELO* dG4 competitor (final concentration at 100 nM). (C) and (D) Similar set up to (A) and (B) except that BioTASQ v.1 (G4 small molecule ligand) was used. Left panels represent the fluorescence intensity of the supernatant, while right panels represent the recovery of fluorescence intensity. Pulldown efficiencies of the L-aptamer for FAM-*hTERC* rG4 with or without the presence of a 1× unlabelled D-*hTELO* dG4 competitor are similar. However, BioTASQ v.1 binds to both D-*hTELO* dG4 and *hTERC* rG4, which greatly affected the pulldown efficiency for FAM-*hTERC* rG4 in the presence of an unlabelled competitor. Error bars indicate the standard deviation from three independent replicates.

a comparable fluorescence recovery (Fig. 4 and Fig. S12, ESI†) when compared to the recovery at different concentrations of L-aptamer in non-competitive assay (Fig. 3H), suggesting that the presence and the quantity of non-targets, whether they bind or do not bind with L-Apt.4-1c, do not significantly affect the pulldown efficiency for FAM-*hTERC* rG4 shown by Biotin-L-Apt.4-1c. Therefore, the pulldown of Biotin-L-Apt.4-1c is specific for rG4 and likely dependent on the binding affinity.

To comprehensively examine the effect of non-structured competitors, we incubated Biotin-L-Apt.4-1c with FAM-*hTERC* rG4 in the presence of a mixture of 1× unlabelled poly rA, rC, and rU. The final concentration of each non-structured competitor in the mixture was 100 nM. The results showed a similar decreasing trend in the fluorescence intensity for the supernatant (Fig. S14A, ESI†) and an increasing trend for recovery (2.68 ± 1.06% to 38.5 ± 1.66%) in the range of 2.5 to 120 nM Biotin-L-Apt.4-1c upon binding to FAM-*hTERC* rG4 in the presence of non-structured competitors (Fig. S14B, ESI†). In the range of 300 to 1600 nM Biotin-L-Apt.4-1c, the recovery of fluorescence intensity gradually reached saturation at 62.2 ± 2.13%, which is also similar to the presence of either 1× or 10× unlabelled *hTELO* dG4 (Fig. 4 and Fig. S13, ESI†). Our results demonstrated that, despite the presence of 1× or 10× non-target competitors, Biotin-L-Apt.4-1c exhibits excellent efficacy in pulling down FAM-*hTERC* rG4. These findings further highlight the utility of the L-Apt.4-1c pulldown assay by providing additional evidence of the selectivity and sensitivity of Biotin-Apt.4-1c towards FAM-*hTERC* rG4.

Comparison of L-Apt.4-1c and BioTASQ v.1 in terms of pulldown efficacy

To compare the isolating ability of Biotin-L-Apt.4-1c and the biotinylated G4 small molecule ligands for FAM-*hTERC* rG4, we performed both non-competitive and competitive assays using a biotinylated G4 small molecule ligand to pulldown FAM-*hTERC* rG4. BioTASQ v.1, a biotinylated ligand known to isolate G4s,[12] was employed as the representative of a G4 small molecule ligand in our assay. First, we performed an MST assay to determine the binding affinity for both BioTASQ v.1-*hTERC* rG4 and BioTASQ v.1-*hTELO* dG4 interactions, and the K_d values were found to be 225 ± 61.5 nM (Fig. S15A, ESI†) and 226 ± 47.7 nM (Fig. S15B, ESI†). Different from L-Apt.4-1c, BioTASQ v.1 showed a similar binding affinity towards both *hTERC* rG4 and *hTELO* dG4, but about 3 times weaker than that of Biotin-L-Apt.4-1c. To verify the ability of G4 ligands to isolate their binding targets, we conducted a non-competitive assay. However, the results showed a weak increasing trend to isolate either *hTERC* rG4 or *hTELO* dG4 with increasing concentration of BioTASQ v.1, which is at 30.6 ± 7.93% (Fig. S16, ESI†) and 13.8 ± 1.68% (Fig. S17, ESI†) at 1600 nM, respectively. Our results revealed that the isolating ability of the L-aptamer was approximately twice that of BioTASQ v.1 (Fig. 3H); therefore, we concluded that the pulldown efficacy for either dG4 or rG4 using BioTASQ v.1 was poor upon binding. As a control, we performed the same experiment on a RNA hairpin, and no binding was found with approximately 0% of the recovery of fluorescence intensity (Fig. S18, ESI†), which verified that BioTASQ v.1 can only distinguish rG4 and dG4. As a second control, we also conducted a competitive pulldown assay to assess whether BioTASQ v.1 specifically isolates FAM-*hTERC* rG4 in the presence of unlabelled *hTELO* dG4 (1× and 10×) and non-G4 competitors (a mixture of poly rA, rC, and rU). Compared to the absence of unlabelled *hTELO* dG4 (Fig. S17, ESI†), the presence of 1× and 10× unlabelled *hTELO* dG4 competitors recovered 22.9 ± 6.04% (Fig. 4) and 17.3 ± 6.84% (Fig. S13, ESI†) of fluorescence intensity, suggesting that the pulldown efficiency is slightly affected by the amount of dG4 competitor. However, the pulldown efficiency for FAM-*hTERC* rG4 shown by BioTASQ v.1 in the presence of a mixture of non-G4s (45.5 ± 4.90%) (Fig. S19, ESI†) is comparable to that of the absence of unlabelled competitors (30.6 ± 7.93%) (Fig. S16, ESI†). It is reasoned that *hTERC* rG4 (target) and *hTELO* dG4 (competitor) have a similar K_d value to BioTASQ v.1, and hence a larger amount of competitor (10×) with a similar affinity would greatly interfere with the pulldown efficiency. Our approach suggested that L-Apt.4-1c competes with state-of-the-art G4 small molecule ligands while offering its specificity to general rG4s even in the presence of dG4, providing great potential to substitute small molecule G4 ligands in further investigations into rG4s based on our new approach.

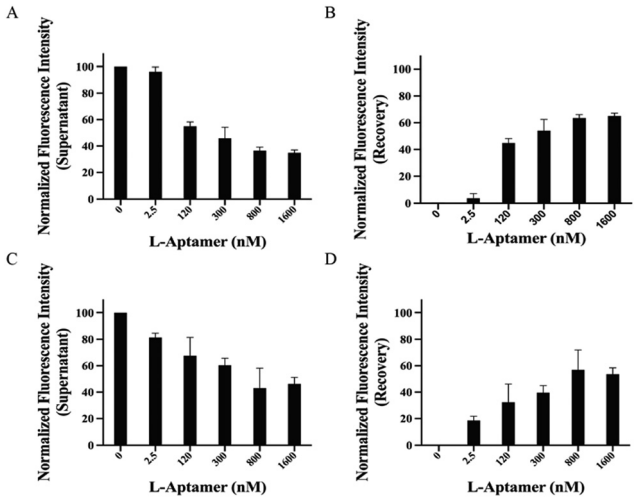

Fig. 5 Pulldown efficiency for FAM-D-*hTERC* rG4 was shown by Biotin-L-Apt.4-1c in complex media. Competitive pulldown assay (A) and (B) performed in the presence of 5 μg of total RNA and (C) and (D) performed in the presence of 3.4 μg of the cell lysate. Left panels present the fluorescence intensity of the supernatant, while right panels present the recovery of fluorescence intensity. In complex media, the pulldown efficiency for FAM-D-*hTERC* rG4 shown by Biotin-L-Apt.4-1c is similar to that of simple buffer. Error bars indicate the standard deviation from three independent replicates.

Evaluation of the binding capacity of L-Apt.4-1c in complex media

To mimic the isolation of specific rG4 using L-aptamers under physiological conditions, we carried out an extensive investigation in two distinctive media as competitors, including total RNA and the cell lysate. First, total RNA represents the collection of all RNA molecules, including ribosomal RNAs (rRNAs), messenger RNAs (mRNAs), and other non-coding RNAs (ncRNAs), which provides valuable information about the potential impact of cellular RNA molecules on the isolation efficiency for *hTERC* rG4 using L-Apt.4-1c. We found that 49.7 ± 16.3% fluorescence recovery was observed at 1600 nM 5′-Biotin-L-Apt.4-1c in the presence of total RNA (Fig. 5A and B). This result showed that L-Apt.4-1c is highly selective for *hTERC* rG4 in a complex mixture of different RNA species. To assess whether L-Apt.4-1c isolates *hTERC* rG4 in a biologically relevant solution, we employed the cell lysate as a competitor, a mixture of cellular components, including metabolites, nucleic acids, proteins, *etc.* Our result showed that 53.6 ± 4.84% of fluorescence recovery was observed at 1600 nM 5′-Biotin-L-Apt.4-1c in the presence of cell lysate (Fig. 5C and D). Interestingly, the fluorescence recovery was comparable to the presence of 10× *hTELO* dG4 (56.7 ± 16.1%) (Fig. S13, ESI†), indicating that the interaction between 5′-Biotin-L-Apt.4-1c and FAM *hTERC* rG4 is not significantly inhibited in various biological media. However, total RNA and the cell lysate are two complex media that contain RNA of different sizes, sequences and structures, along with other biomolecules in the case of cell lysate. To further verify the effectiveness of pulldown by Biotin-L-Apt.4-1c, *hTERC* rG4 and *APP* rG4 enrichment was monitored among several rG4s in the endogenous pulldown (in either total RNA or the cell lysate) using Biotin-L-Apt.4-1c, followed by RT-qPCR. In total RNA pulldown, *hTERC* rG4 and *APP* rG4 were determined at threshold cycles (Ct) of 25.3 cycles and 23.4 cycles (Fig. S20A, ESI†), respectively. To compare the rG4 enrichment, endogenous pulldown was also performed using the biotin-L-mutant, which yielded much larger Ct values of >40 and 38.7 cycles, respectively. The large difference in Ct values indicated that rG4s can be enriched using Biotin-L-Apt.4-1c. Similarly, the *hTERC* rG4 and *APP* rG4 in cell lysate pulldown also showed enrichment, albeit weaker, with Ct values of 26.3 and 25.7 cycles using Biotin-L-Apt.4-1c and 28.6 and 28.0 cycles using the biotin-L-mutant (Fig. S20B, ESI†). It is likely that cell lysate samples are more complex in nature, and therefore the enrichment observed is less obvious than that observed using total RNA samples. To sum up, our approach can specifically pulldown rG4 using the L-aptamer from both simple buffer and complex media with the evidence of both competitive pulldown analysis and RT-qPCR results, and this result has significant implications for further investigation of rG4 structures in diverse systems.

Conclusion

In conclusion, this work developed a magnetic-bead based pulldown platform by leveraging L-Apt.4-1c as a general rG4 binder with high affinity and specificity. Our platform allows both non-competitive and competitive analyses for the interaction between rG4 targets (or non-rG4 targets) and the L-aptamer (or G4 small molecule ligands). Furthermore, we also investigated the endogenous pulldown efficiency for *hTERC* rG4 using Biotin-L-Apt.4-1c, demonstrating its ability to enrich the target rG4 from total RNA or the cell lysate. In the future, L-aptamers can also be generated using efficient SELEX-based approaches, such as rG4-SELEX[38] and G4-SELEX-seq,[42] which typically require a few rounds of selection, and the resultant L-aptamer can be functionalized for affinity capture or isolation, as well as for other applications such as imaging. To sum up, our findings indicate that L-Apt.4-1c exhibits superior pulldown efficiency and specificity for general rG4s compared to BioTASQ v.1. This work provides a valuable platform for the identification and characterization of rG4s and shows the capability for further enhancing the potential of L-aptamers as highly promising molecular tools for exploring and understanding the rG4 structure in a transcript-specific and transcriptome-wide manner.

Data availability

The data underlying this article are available in the article and in the ESI.† Further data will be shared upon reasonable request to the corresponding author.

Conflicts of interest

The authors declare that they have no conflicts of interest.

Acknowledgements

This work was supported by the NSFC Excellent Young Scientists Fund (Hong Kong and Macau) Project [32222089]; Research Grants Council of the Hong Kong SAR, China Projects [CityU 11100123, CityU 11100222, CityU 11100421]; Croucher Foundation Project [9509003]; State Key Laboratory of Marine Pollution Seed Collaborative Research Fund [SCRF/0037, SCRF/0040, SCRF/0070]; and City University of Hong Kong projects [7030001, 6000827, 9678302] to C. K. K. We thank Prof. David Monchaud for sharing the BioTASQ v.1 ligand.

Notes and references

1 J. T. Davis, *Angew. Chem., Int. Ed.*, 2004, **43**, 668–698.
2 C. K. Kwok and C. J. Merrick, *Trends Biotechnol.*, 2017, **35**, 997–1013.
3 F. Dumetz, E. Y. Chow, L. M. Harris, S. W. Liew, A. Jensen, M. I. Umar, B. Chung, T. F. Chan, C. J. Merrick and C. K. Kwok, *Nucleic Acids Res.*, 2021, **49**, 12486–12501.
4 X. Yang, J. Cheema, Y. Zhang, H. Deng, S. Duncan, M. I. Umar, J. Zhao, Q. Liu, X. Cao, C. K. Kwok and Y. Ding, *Genome Biol.*, 2020, **21**, 226.
5 X. Shao, W. Zhang, M. I. Umar, H. Y. Wong, Z. Seng, Y. Xie, Y. Zhang, L. Yang, C. K. Kwok and X. Deng, *mBio*, 2020, **11**(1), e02926-19.
6 X. Chen, J. Yuan, G. Xue, S. Campanario, D. Wang, W. Wang, X. Mou, S. W. Liew, M. I. Umar, J. Isern, Y. Zhao, L. He, Y. Li, C. J. Mann, X. Yu, L. Wang, E. Perdiguero, W. Chen, Y. Xue, Y. Nagamine, C. K. Kwok, H. Sun, P. Munoz-Canoves and H. Wang, *Nat. Commun.*, 2021, **12**, 5043.
7 N. Bohalova, A. Cantara, M. Bartas, P. Kaura, J. Stastny, P. Pecinka, M. Fojta and V. Brazda, *Int. J. Mol. Sci.*, 2021, **22**, 3433.
8 G. Qin, C. Zhao, Y. Liu, C. Zhang, G. Yang, J. Yang, Z. Wang, C. Wang, C. Tu, Z. Guo, J. Ren and X. Qu, *Cell Discovery*, 2022, **8**, 86.
9 R. Hansel-Hertsch, D. Beraldi, S. V. Lensing, G. Marsico, K. Zyner, A. Parry, M. Di Antonio, J. Pike, H. Kimura, M. Narita, D. Tannahill and S. Balasubramanian, *Nat. Genet.*, 2016, **48**, 1267–1272.
10 L. M. Harris and C. J. Merrick, *PLoS Pathog.*, 2015, **11**, e1004562.
11 R. Hänsel-Hertsch, M. Di Antonio and S. Balasubramanian, *Nat. Rev. Mol. Cell Biol.*, 2017, **18**, 279–284.
12 S. Muller, S. Kumari, R. Rodriguez and S. Balasubramanian, *Nat. Chem.*, 2010, **2**, 1095–1098.
13 T. Santos, G. F. Salgado, E. J. Cabrita and C. Cruz, *Pharmaceuticals*, 2021, 14.
14 K. H. Ngo, R. Yang, P. Das, G. K. T. Nguyen, K. W. Lim, J. P. Tam, B. Wu and A. T. Phan, *Chem. Commun.*, 2020, **56**, 1082–1084.
15 H. Fernando, S. Sewitz, J. Darot, S. Tavare, J. L. Huppert and S. Balasubramanian, *Nucleic Acids Res.*, 2009, **37**, 6716–6722.
16 H. Fernando, R. Rodriguez and S. Balasubramanian, *Biochemistry*, 2008, **47**, 9365–9371.
17 G. Biffi, D. Tannahill, J. McCafferty and S. Balasubramanian, *Nat. Chem.*, 2013, **5**, 182–186.
18 S. M. Javadekar, N. M. Nilavar, A. Paranjape, K. Das and S. C. Raghavan, *DNA Res.*, 2020, **27**, 1–17.
19 X. Mou and C. K. Kwok, *J. Am. Chem. Soc.*, 2023, **145**, 18693–18697.
20 P. M. Yangyuoru, M. Di Antonio, C. Ghimire, G. Biffi, S. Balasubramanian and H. Mao, *Angew. Chem.*, 2015, **127**, 924–927.
21 A. Henderson, Y. Wu, Y. C. Huang, E. A. Chavez, J. Platt, F. B. Johnson, R. M. Brosh, Jr., D. Sen and P. M. Lansdorp, *Nucleic Acids Res.*, 2017, **45**, 6252.
22 B. Heddi, V. V. Cheong, H. Martadinata and A. T. Phan, *Proc. Natl. Acad. Sci. U. S. A.*, 2015, **112**, 9608–9613.
23 S. Xu, Q. Li, J. Xiang, Q. Yang, H. Sun, A. Guan, L. Wang, Y. Liu, L. Yu, Y. Shi, H. Chen and Y. Tang, *Sci. Rep.*, 2016, **6**, 24793.
24 J. Ren, H. Qin, J. Wang, N. W. Luedtke, E. Wang and J. Wang, *Anal. Bioanal. Chem.*, 2011, **399**, 2763–2770.
25 H. Arthanari, S. Basu, T. L. Kawano and P. H. Bolton, *Nucleic Acids Res.*, 1998, **26**, 3724–3728.
26 R. Rodriguez, S. Müller, J. A. Yeoman, C. Trentesaux, J.-F. Riou and S. Balasubramanian, *J. Am. Chem. Soc.*, 2008, **130**, 15758–15759.
27 M. Nikan and J. C. Sherman, *Angew. Chem., Int. Ed.*, 2008, **47**, 4900–4902.
28 F. R. Sperti, T. Charbonnier, P. Lejault, J. Zell, C. Bernhard, I. E. Valverde and D. Monchaud, *ACS Chem. Biol.*, 2021, **16**, 905–914.
29 I. Renard, M. Grandmougin, A. Roux, S. Y. Yang, P. Lejault, M. Pirrotta, J. M. Y. Wong and D. Monchaud, *Nucleic Acids Res.*, 2019, **47**, 5502–5510.
30 F. Sperti Rota, T. Charbonnier, P. Lejault, J. Zell, C. Bernhard, I. E. Valverde and D. Monchaud, *ACS Chem. Biol.*, 2021, **16**, 905–914.
31 A. Ozer, J. M. Pagano and J. T. Lis, *Mol. Ther.--Nucleic Acids*, 2014, **3**, e183.
32 A. B. Iliuk, L. Hu and W. A. Tao, *Anal. Chem.*, 2011, **83**, 4440–4452.
33 A. V. Lakhin, V. Z. Tarantul and L. V. Gening, *Acta Naturae*, 2013, **5**, 34–43.
34 P. Rothlisberger and M. Hollenstein, *Adv. Drug Delivery Rev.*, 2018, **134**, 3–21.
35 D. Ji, H. Feng, S. W. Liew and C. K. Kwok, *Trends Biotechnol.*, 2023, 1360–1384.
36 J. P. Elskens, J. M. Elskens and A. Madder, *Int. J. Mol. Sci.*, 2020, 21.
37 B. E. Young, N. Kundu and J. T. Sczepanski, *Chemistry*, 2019, **25**, 7981–7990.
38 C. Y. Chan and C. K. Kwok, *Angew. Chem., Int. Ed.*, 2020, **59**, 5293–5297.
39 M. I. Umar and C. K. Kwok, *Nucleic Acids Res.*, 2020, **48**, 10125–10141.
40 H. Zhao, H. Y. Wong, D. Ji, K. Lyu and C. K. Kwok, *ACS Appl. Mater. Interfaces*, 2022, **14**, 30582–30594.
41 C.-Y. Chan and C. K. Kwok, *Angew. Chem., Int. Ed.*, 2020, **59**, 5293–5297.
42 D. Ji, J. H. Yuan, S. B. Chen, J. H. Tan and C. K. Kwok, *Nucleic Acids Res.*, 2023, **51**, 11439–11452.